UDC 519.635.4
IRSTI 27.35.16

https://doi.org/10.55452/1998-6688-2026-23-1-265-280

[1]*Sinitsa A.V.,
PhD, Assistant Professor, ORCID ID: 0000-0002-5828-7820,
*e-mail: a.sinitsa@kbtu.kz.
[1]Shkorko A.K.,
MSc, Lecturer, ORCID ID: 0009-0003-0402-4720,
e-mail: a.ukassova@kbtu.kz.
[1]Tskhay Y.A.,
MSc, Lecturer, ORCID ID: 0009-0003-0772-4319,
e-mail: y.tskhay@kbtu.kz.
[2]Karduck A.P.,
PhD, Professor, ORCID ID: 0000-0002-8142-6710,
e-mail: achim.karduck@hs-furtwangen.de

[1]Kazakh-British Technical University, Almaty, Kazakhstan
[2]Hochschule Furtwangen University, Furtwangen, Germany

VARIATIONAL APPROACH FOR IDENTIFYING ENVIRONMENTAL PARAMETERS VIA INVERSE ANALYSIS OF ACOUSTIC WAVE PROPAGATION

Abstract

This paper presents a numerical method for reconstructing the spatial distribution of sound speed in inhomogeneous media based on the inverse analysis of acoustic wave propagation. The mathematical model relies on the second-order wave equation with variable coefficients. The inverse problem is formulated as an optimization task to minimize the residual functional between simulated and observed pressure data at the domain boundaries. To efficiently calculate the gradient of the functional, an adjoint (auxiliary) problem method is employed, derived via variational calculus. The numerical implementation is performed using an explicit finite-difference scheme. Computational experiments on a one-dimensional model of a heterogeneous medium (soil-metal-soil) demonstrate that the proposed algorithm allows for reliable reconstruction of the velocity profile, particularly in zones of sharp contrast. The study analyzes the sensitivity of the solution and the convergence rate, showing that 500 iterations provide an optimal balance between accuracy and computational cost.

Keywords: inverse problem, acoustic wave equation, adjoint state method, parameter identification, gradient descent, finite-difference method.

Received: January 30, 2026; revised : March 5, 2026; March 10, 2026; accepted: March 13, 2026.

Introduction

Acoustic wave propagation modeling is a cornerstone of modern scientific and engineering applications, ranging from geophysical exploration and seismology to medical diagnostics and architectural acoustics [1, 2]. While the direct problem of predicting wave behavior in a known medium is well-established, the inverse problem, identifying the physical properties of the medium, such as sound speed or density, from observed wave fields, remains a significant mathematical and computational challenge. These problems are critical for non-destructive testing, environmental monitoring, and the identification of subsurface structures [3, 4]. Inverse problems in acoustics and wave propagation are typically ill-posed in the sense of Hadamard: solutions may not exist, may not

be unique, or may not depend continuously on the input data [5]. This instability necessitates the use of robust numerical methods, regularization techniques, and advanced optimization strategies. The fundamental theory of ill-posed problems has been extensively developed by the global scientific community, with pioneering contributions from A.N. Tikhonov, M.M. Lavrentiev and V.G. Romanov [6–8]. In Kazakhstan, the theory of inverse problems has a strong tradition and has been significantly advanced by the scientific school of Academician S.I. Kabanikhin. His works on optimization methods for hyperbolic inverse problems provide a crucial theoretical framework for gradient-based reconstruction [9, 10]. Building on this foundation, B. Rysbaiuly has made notable contributions to the numerical solution of coefficient inverse problems. In particular, his recent studies on heat conduction and moisture transfer equations demonstrate the efficacy of finite-difference schemes and iterative regularization in determining unknown coefficients in layered media [11, 12]. Similarly, Zh. Karashbayeva has developed efficient methods for solving boundary inverse problems for systems of transfer equations, focusing on the iterative determination of boundary regimes and medium parameters [13]. These domestic studies collectively form a solid methodological basis for applying variational approaches to complex physical models. Parallel to these theoretical developments, applied research in wave propagation has evolved significantly. K.T. Iskakov and M.A. Bektemesov have proposed parallel algorithms for solving inverse wave problems, which are particularly relevant for large-scale geophysical applications [14, 15]. In the context of acoustics, recent advances involve the use of the Adjoint State Method (ASM). As highlighted by Plessix and Virieux, ASM allows for the efficient computation of the gradient of the residual functional, making it feasible to solve high-dimensional optimization problems such as Full-Waveform Inversion (FWI) [16, 17]. Despite these advances, reconstructing sharp contrasts in heterogeneous media (e.g., ore bodies in soil) remains computationally expensive and sensitive to noise. Traditional gradient-based methods often suffer from slow convergence or entrapment in local minima [18]. Therefore, there is a continuous need to refine variational algorithms and integrate them with stable difference schemes. In this paper, we propose a variational approach for identifying the sound speed profile in a one-dimensional heterogeneous medium. We derive the adjoint problem and the gradient of the residual functional using variational calculus. The proposed method is implemented using an explicit finite-difference scheme and validated through numerical experiments on a “soil-metal-soil” model. This work extends the variational framework discussed in and complements the findings of by applying them to the specific context of acoustic impedance identification [11–14, 19].

Mathematical Formulation of the Direct Problem

The propagation of acoustic waves in a three-dimensional inhomogeneous medium is governed by the second-order scalar wave equation:

$$\frac{\partial^2 p}{\partial t^2} = \nabla \cdot (c^2(\vec{x})\nabla p). \tag{1}$$

Where $p(\vec{x},t)$ is the acoustic pressure and $c(\vec{x})$ is the variable speed of sound, $\vec{x} = (x,y,z)$. Considering the possible inhomogeneity of the medium (the variable speed of sound $c = c(x,y,z)$) , the wave process is described by the following differential model:

$$\frac{\partial^2 p}{\partial t^2} = \frac{\partial}{\partial x}\left(c^2 \frac{\partial p}{\partial x}\right) + \frac{\partial}{\partial y}\left(c^2 \frac{\partial p}{\partial y}\right) + \frac{\partial}{\partial z}\left(c^2 \frac{\partial p}{\partial z}\right). \tag{2}$$

Where $p = p(x,y,z,t)$ is the acoustic pressure, $c = c(x,y,z)$ is the speed of sound in the medium, depending on the spatial coordinates ($\Omega = [0,L_x]\times[0,L_y]\times[0,L_z]\times[0,T_m]$). This equation is a linear hyperbolic problem with variable coefficients and is the basis for setting direct and inverse acoustic problems.

In this paper, we use absorbing boundary conditions that model the interaction of the medium with the external space. These conditions are designed to minimize the reflection of waves from the boundaries of the modeling domain, thereby bringing the conditions closer to open or infinite space. The boundary conditions have the following form:

$$\begin{cases} c^2 \dfrac{\partial p}{\partial x}\Big|_{x=0} = \dfrac{1}{\zeta_x}\left(p_{w,x} - p(x,y,z,t)\right)\Big|_{x=0}, \\ c^2 \dfrac{\partial p}{\partial x}\Big|_{x=L_x} = -\dfrac{1}{\zeta_{L_x}}\left(p_{w,L_x} - p(x,y,z,t)\right)\Big|_{x=L_x}, \\ c^2 \dfrac{\partial p}{\partial y}\Big|_{y=0} = \dfrac{1}{\zeta_y}\left(p_{w,y} - p(x,y,z,t)\right)\Big|_{y=0}, \\ c^2 \dfrac{\partial p}{\partial y}\Big|_{y=L_y} = -\dfrac{1}{\zeta_{L_y}}\left(p_{w,L_y} - p(x,y,z,t)\right)\Big|_{y=L_y}, \\ c^2 \dfrac{\partial p}{\partial z}\Big|_{z=0} = \dfrac{1}{\zeta_z}\left(p_{w,z} - p(x,y,z,t)\right)\Big|_{z=0}, \\ c^2 \dfrac{\partial p}{\partial z}\Big|_{z=L_z} = -\dfrac{1}{\zeta_{L_z}}\left(p_{w,L_z} - p(x,y,z,t)\right)\Big|_{z=L_z}. \end{cases} \quad (3)$$

Here ζ denotes the absorption coefficient, which characterizes the ability of the environment at the boundaries to weaken or transmit acoustic pressure without reflection. The smaller the value of ζ, the stronger the influence of the external environment on the field inside the computational domain. The values p_w are known or approximate values of sound pressure in a medium near a boundary. In this paper, the following initial configuration is considered:

$$\begin{cases} p|_{t=0} = p_0, \\ \dfrac{\partial p}{\partial t}\Big|_{t=0} = 0. \end{cases} \quad (4)$$

Here p_0 is the given pressure distribution at the initial moment of time, which are the given constant values at each point. The second condition corresponds to the situation when at the initial moment the medium is at rest, i.e. the rate of pressure change over time is absent.

Table 1 – Physical parameters

Notation	Description	Units of Measurement
L_x, L_y, L_z	spatial boundary points of enclosure	$[m]$
T_m	considered time interval	[s]
Ω	investigated three-dimensional non-stationary domain	$[m^3 \times s]$
$p(x,y,z,t)$	sound pressure	$[Pa]$
c	referenced speed of sound	$\left[\frac{m}{s}\right]$
ζ	sound absorption coefficient	[ ]

1D Reduction of the direct problem

Since the computational experiments are performed on a 1D domain, we reduce the general 3D wave equation to the one-dimensional form. Setting $p = p(x,t)$ and $c = c(x)$, equation (2) reduces to:

$$\frac{\partial^2 p}{\partial t^2} = \frac{\partial}{\partial x}\left(c^2(x)\frac{\partial p}{\partial x}\right) + f(x,t), \quad x \in (0,L), \quad t \in (0,T). \quad (5)$$

where $f(x,t)$ is the acoustic source term (defined explicitly in Section 3 below), $L = 1$ m is the domain length, and T is the total simulation time. The absorbing boundary conditions (3) reduce to:

$$c^2 \frac{\partial p}{\partial x}\Big|_{x=0} = \frac{1}{\zeta_0}\left(p_{w,0} - p(0,t)\right), \tag{6}$$

$$c^2 \frac{\partial p}{\partial x}\Big|_{x=L} = -\frac{1}{\zeta_L}\left(p_{w,L} - p(L,t)\right). \tag{7}$$

The initial conditions remain:

$$p(x,0) = p_0(x), \qquad \frac{\partial p}{\partial t}(x,0) = 0. \tag{8}$$

The acoustic source is modeled as a Gaussian pulse in space and time, introduced as an additive forcing term in equation (5):

$$f(x,t) = A_0 \exp\left(-\frac{(x - x_s)^2}{2\sigma_x^2}\right) \exp\left(-\frac{(t - t_0)^2}{2\sigma_t^2}\right), \tag{9}$$

where:

- $A_0 = 1.0$ is the source amplitude,
- $x_s = 5\,\Delta x = 0.05$ m is the source location (node index 5),
- $\sigma_x = \Delta x$ is the spatial width of the pulse,
- $t_0 = 3\sigma_t$ is the time delay (ensuring the pulse starts near zero),
- $\sigma_t = 3\,\Delta t$ is the temporal width.

This concentrated source generates a broad-spectrum wavelet that propagates through the heterogeneous medium and reflects off the impedance contrasts at the inclusion boundaries ($x = 0.4$ m and $x = 0.6$ m).

Formulation of the Inverse Problem

Direct problem: Given $c(x)$, find $p(x,t)$ satisfying (5), (6), (7), (8).

Inverse problem: Given the measured boundary pressure data $p_s(0,t)$ and $p_s(L,t)$ for $t \in [0,T]$, find the function $c(x) \in C_{ad}$ that minimizes the residual functional:

$$J(c^2) = \frac{1}{2}\int_0^T \left[(p(0,t;c) - p_s(0,t))^2 + (p(L,t;c) - p_s(L,t))^2\right] dt, \tag{10}$$

subject to the state constraint that p satisfies the direct problem (5)–(8).

The parameter space is restricted to the admissible set:

$$C_{ad} = \{c \in L^\infty(0,L) : c_{\min} \le c(x) \le c_{\max}\}, \tag{11}$$

where $c_{\min} = 100$ m/s and $c_{\max} = 6000$ m/s are physically motivated bounds. This constraint is enforced at every gradient-descent update step via projection:

$$c_{n+1}^2(x) = \mathrm{Proj}_{c_{ad}}[c_n^2(x) - \gamma_n \nabla_{c^2} J(x)]. \tag{12}$$

Variational Formulation and Adjoint Problem

The inverse problem aims to find $c(x)$ that minimizes the residual functional $J(c)$, defined as the squared difference between calculated pressure p and measured pressure p_s at the boundaries:

$$J(c) = \int_0^T \sum_{x \in \{0,L\}} \left(p(x,t;c) - p_s(x,t)\right)^2 dt\,. \tag{13}$$

To calculate the gradient of J with respect to c^2, we introduce the adjoint state $\psi(x,t)$. The function ψ is used for scalar multiplication (in the sense of the inner product in the pre-Hilbert space) of the original differential equation, after which integration is performed over the entire domain $\Omega = [0, L_x] \times [0, T_m]$. We are using the special functional which is the mapping from one metric space to another represented as Pre-Hilbert space with the following inner product:

$$\langle f, g \rangle = \int (f \cdot g) d\Omega = \int_0^{L_x} \int_0^{T_m} (f \cdot g)\, dt\, dx. \tag{14}$$

By multiplying the state equation by Ψ and integrating by parts over the space-time domain, we derive the adjoint problem for one-dimension case (for three- dimension case similar):

$$\frac{\partial^2 \psi}{\partial t^2} - \frac{\partial}{\partial x}\left(c^2(x)\frac{\partial \psi}{\partial x}\right) = 0. \tag{15}$$

The adjoint problem is solved backwards in time with terminal conditions:

$$\psi(x, T) = 0, \quad \frac{\partial \psi}{\partial t}(x, T) = 0. \tag{16}$$

The boundary conditions for the adjoint variable Ψ are driven by the residual of the direct problem:

$$c^2 \frac{\partial \psi}{\partial n} + \frac{1}{\zeta}\frac{\partial \psi}{\partial t} = 2(p - p_e) \quad \text{on } \partial\Omega. \tag{17}$$

We present the full variational derivation of the adjoint equations (15) – (17) from first principles. Introduce the Lagrangian functional by adjoining the state equation to J via the multiplier $\psi(x,t)$:

$$\mathcal{L}(p, \psi, c^2) = J(c^2) + \int_0^T \int_0^L \psi \left[\frac{\partial^2 p}{\partial t^2} - \frac{\partial}{\partial x}\left(c^2 \frac{\partial p}{\partial x}\right) - f\right] dx\, dt. \tag{18}$$

Consider a perturbation $p \to p + \epsilon\, \delta p$ and set $\frac{d}{d\epsilon}\mathcal{L}|_{\epsilon=0} = 0$. This yields:

$$\delta_p \mathcal{L} = \delta J + \int_0^T \int_0^L \psi \left[\frac{\partial^2 (\delta p)}{\partial t^2} - \frac{\partial}{\partial x}\left(c^2 \frac{\partial (\delta p)}{\partial x}\right)\right] dx\, dt = 0. \tag{19}$$

Integration by parts in time (twice) for the first term:

$$\int_0^T \psi \frac{\partial^2 (\delta p)}{\partial t^2}\, dt = \left[\psi \frac{\partial (\delta p)}{\partial t}\right]_0^T - \left[\frac{\partial \psi}{\partial t}\, \delta p\right]_0^T + \int_0^T \frac{\partial^2 \psi}{\partial t^2}\, \delta p\, dt. \tag{20}$$

Enforcing terminal conditions $\psi(x, T) = 0$ and $\frac{\partial \psi}{\partial t}(x, T) = 0$ (and noting $\delta p(x, 0) = 0$, $\frac{\partial (\delta p)}{\partial t}(x, 0) = 0$ from fixed initial data) eliminates the boundary terms in time.

Integration by parts in space for the second term:

$$-\int_0^T \int_0^L \psi \frac{\partial}{\partial x}\left(c^2 \frac{\partial (\delta p)}{\partial x}\right) dx\, dt =$$

$$\int_0^T \int_0^L \frac{\partial \psi}{\partial x} c^2 \frac{\partial (\delta p)}{\partial x}\, dx\, dt - \int_0^T \left[\psi\, c^2 \frac{\partial (\delta p)}{\partial x}\right]_0^L dt. \tag{21}$$

A second integration by parts in x gives:

$$-\int_0^T \int_0^L \frac{\partial}{\partial x}\left(c^2 \frac{\partial \psi}{\partial x}\right) \delta p\, dx\, dt + \int_0^T \left[c^2 \frac{\partial \psi}{\partial x}\, \delta p - \psi\, c^2 \frac{\partial (\delta p)}{\partial x}\right]_0^L dt. \tag{22}$$

Variation of the Functional J

$$\delta J = \int_0^T \left[\left(p(0,t) - p_e(0,t)\right) \delta p(0,t) + \left(p(L,t) - p_e(L,t)\right) \delta p(L,t)\right] dt. \tag{23}$$

Combining the above, the interior residual gives the adjoint equation:

$$\frac{\partial^2 \psi}{\partial t^2} - \frac{\partial}{\partial x}\left(c^2(x)\frac{\partial \psi}{\partial x}\right) = 0, \quad x \in (0, L), \quad t \in (0, T), \tag{24}$$

solved backward in time with terminal conditions:

$$\psi(x,T) = 0, \qquad \frac{\partial \psi}{\partial t}(x,T) = 0.$$

The boundary terms yield the adjoint boundary conditions (after using the absorbing BC structure of the direct problem):

$$c^2 \frac{\partial \psi}{\partial n}|_{\partial\Omega} + \frac{1}{\zeta}\frac{\partial \psi}{\partial t}|_{\partial\Omega} = 2(p - p_e)|_{\partial\Omega}, \tag{25}$$

where $\frac{\partial}{\partial n}$ denotes the outward normal derivative. This completes the derivation of the adjoint problem.

Gradient Computation

The gradient of the functional (13) with respect to the parameter c^2 is obtained from the interaction between the forward field p and the adjoint field Ψ. Consider the perturbation $c^2 \to c^2 + \epsilon\,\delta(c^2)$. The resulting perturbation of the state equation gives an auxiliary problem for δp:

$$\frac{\partial^2(\delta p)}{\partial t^2} - \frac{\partial}{\partial x}\left(c^2 \frac{\partial(\delta p)}{\partial x}\right) = \frac{\partial}{\partial x}\left(\delta(c^2)\frac{\partial p}{\partial x}\right). \tag{26}$$

Multiplying by ψ and integrating over $\Omega_T = [0, L] \times [0, T]$:

$$\int_0^T \int_0^L \psi \left[\frac{\partial^2(\delta p)}{\partial t^2} - \frac{\partial}{\partial x}\left(c^2 \frac{\partial(\delta p)}{\partial x}\right)\right] dx\,dt = \int_0^T \int_0^L \psi \frac{\partial}{\partial x}\left(\delta(c^2)\frac{\partial p}{\partial x}\right) dx\,dt. \tag{27}$$

The left-hand side vanishes when ψ satisfies the adjoint problem (15) – (17). Integrating the right-hand side by parts in :

$$\int_0^T \int_0^L \psi \frac{\partial}{\partial x}\left(\delta(c^2)\frac{\partial p}{\partial x}\right) dx\,dt =$$

$$= -\int_0^T \int_0^L \frac{\partial \psi}{\partial x}\frac{\partial p}{\partial x}\,\delta(c^2)\,dx\,dt + \text{boundary terms}. \tag{28}$$

The boundary terms are absorbed into the adjoint boundary condition (17). Therefore, the first-order variation of J satisfies:

$$\delta J = \int_0^L \left(-\int_0^T \frac{\partial p}{\partial x}\frac{\partial \psi}{\partial x}\,dt\right)\delta(c^2)\,dx. \tag{29}$$

By the definition of the L^2-gradient, we identify:

$$\nabla_{c^2} J = -\int_0^T \left(\frac{\partial p}{\partial x}\frac{\partial \psi}{\partial x}\right) dt. \tag{30}$$

which is the cross-correlation of the spatial derivatives of the forward and adjoint fields, integrated over time. This expression is computed pointwise at each spatial node after solving both the direct and adjoint problems.

This gradient is used in the iterative update formula:

$$c_{n+1}^2(x) = c_n^2(x) - \gamma_n \nabla_{c^2} J(x). \tag{31}$$

where γ_n is the descent step size. Explicitly the formula obtains the following form:

$$c_{n+1}^2 = c_n^2 - \gamma_n(x)\left(\int_0^T \int_0^{L_x} \left(\frac{\partial p_n}{\partial x}, \frac{\partial \psi}{\partial x}\right) dx\,dt\right). \tag{32}$$

Materials and methods

Numerical Scheme

The continuous equations were discretized using the explicit Finite Difference Method (FDM). For the second-order derivatives in time and space, the standard central difference approximations were used. The update step for pressure p_i^{n+1} (where i is the spatial index and n is the time index) is given by:

$$p_i^{n+1} = \Delta t^2 \left[\frac{c_{i+1/2}^2 (p_{i+1}^n - p_i^n) - c_{i-1/2}^2 (p_i^n - p_{i-1}^n)}{\Delta x^2} \right] + 2p_i^n - p_i^{n-1}. \quad (33)$$

The stability of the explicit scheme is ensured by the Courant–Friedrichs–Lewy (CFL) condition:

$$CFL = \frac{c_{max} \Delta t}{\Delta x} \leq 1. \quad (34)$$

the stability of the scheme must be maintained as $c(x)$ evolves. We address this as follows:

Step-size constraint. At each iteration n, the updated profile is projected onto the admissible set:

$$c_{n+1}^2(x) = \min \left(c_{\max}^2, \max(c_{\min}^2, c_n^2(x) - \gamma_n \nabla_{c^2} J(x)) \right), \quad (35)$$

with $c_{\max} = 6000$ m/s and $c_{\min} = 100$ m/s. The time step Δt is fixed once, based on $c_{\max}$:

$$\Delta t = \frac{\mathrm{CFL} \cdot \Delta x}{c_{\max}}, \quad \mathrm{CFL} = 0.5. \quad (36)$$

Since $c_n(x) \leq c_{\max}$ is enforced by projection at every iteration, the CFL condition (34) is satisfied throughout the inversion, regardless of the gradient updates.

In our experiments, we set $CFL = 0.5$. This approach allows preserving the symmetry of the computational scheme, ensuring correct conjugation between the direct and inverse problems and, as a result, increasing the accuracy and stability of the numerical method as a whole.

$$\psi_i^{n+1} = \Delta t^2 \left(c_{n_{i+\frac{1}{2}}}^2 \frac{\psi_{i+1}^n - \psi_i^n}{\Delta x^2} - c_{n_{i-\frac{1}{2}}}^2 \frac{\psi_i^n - \psi_{i-1}^n}{\Delta x^2} \right) + 2\psi_i^n - \psi_i^{n-1} \quad (37)$$

Where: $c_{n_{i+\frac{1}{2}}}^2 = \frac{c_{n_{i+1}}^2 + c_{n_i}^2}{2}$; $c_{n_{i-\frac{1}{2}}}^2 = \frac{c_{n_{i-1}}^2 + c_{n_i}^2}{2}$.

Simulation Setup

The choice of a one-dimensional formulation of the problem is determined by both methodological and computational considerations. Even though real media are usually three-dimensional in nature, the direct and especially the inverse problems in multidimensional formulations are accompanied by a sharp increase in computational complexity, memory volumes, and time costs. Solving the inverse problem in the three-dimensional domain requires resources comparable to high-performance computing clusters and significantly complicates the sensitivity analysis and interpretation of the results.

The algorithm was implemented in Python. The computational domain was defined as a 1D segment of length $L = 1$ m, discretized into 100 nodes ($\Delta x = 0.01$ m).

- True Model: A heterogeneous medium consisting of three layers:
  - $x \in [0,0.4]$: Soil ($c = 1500$ m/s)
  - $x \in [0.4, 0.6]$: Metal inclusion ($c = 3000$ m/s)
  - $x \in [0.6,1.0]$: Soil ($c = 1500$ m/s)
- Source: A Gaussian pulse source located at node 5.
- Time Domain: Total time $T = 0.01$ s, divided into 3000 time steps.

◆ Input Data: "Measured" pressure p_e was generated by solving the forward problem with the true velocity profile.

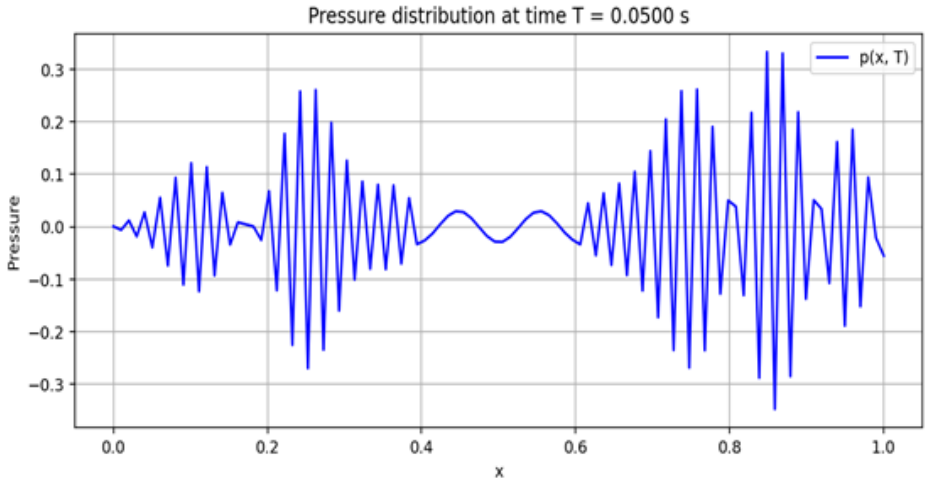

Figure 1 – Propagation of sound pressure in the simulation domain with the true sound velocity profile

Figure 1 shows the distribution of acoustic pressure $p(x,T)$ along the entire simulation area at a fixed time $T = 0.05\ s$. This field is the basis for calculating the gradient in the problem of reverse recovery of the profile $c(x)$.

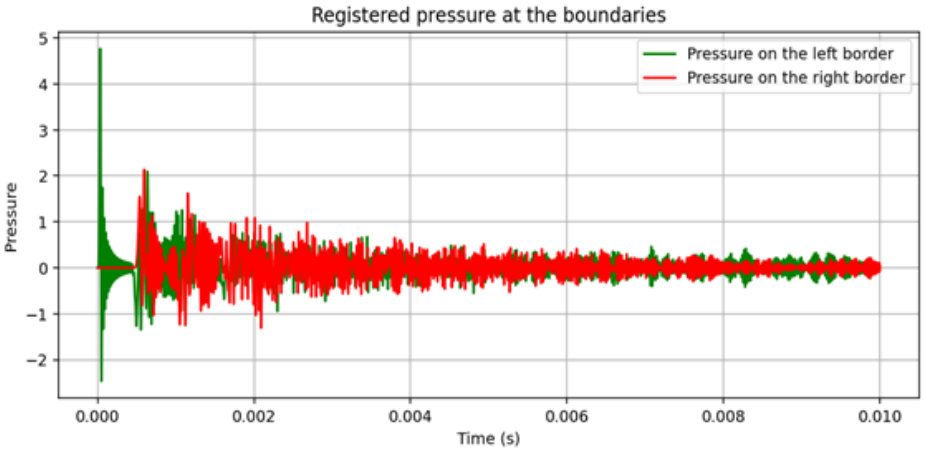

Figure 2 – The pressure recorded over time at the boundaries of the region

Figure 2 shows the time dependence of the pressure recorded at the left (green line) and right (red line) boundaries of the medium

Inversion Procedure

The inversion started with a homogeneous initial guess $c_{init}(x) = 1500$ m/s. The optimization loop consisted of:

Solving the forward problem with current $c(x)$.

Computing residuals at boundaries ($x = 0, x = L$).

Solving the adjoint problem backward in time using the residuals as sources.

Computing the gradient by integrating the product of spatial derivatives of p and ψ.

Updating $c(x)$ using the gradient descent method with a fixed step size $\gamma = 10^{-6}$.

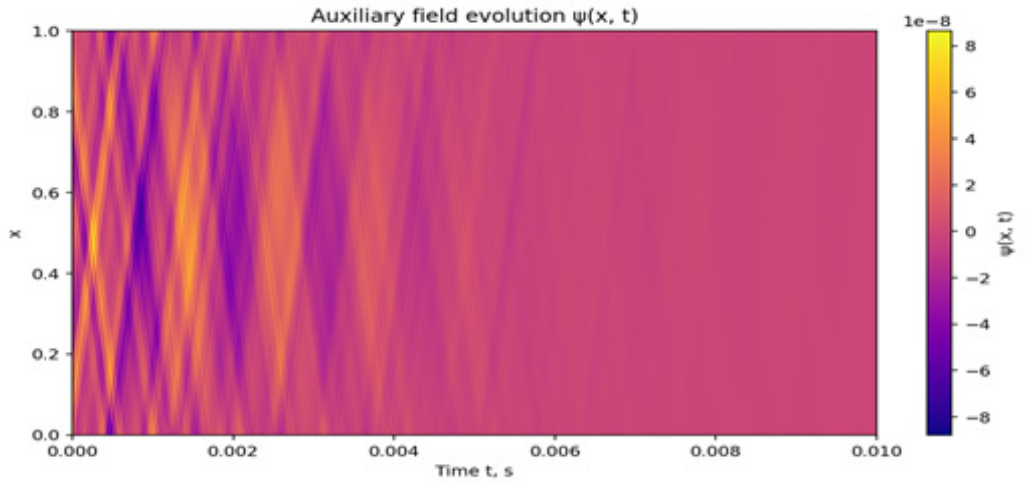

Figure 3 – The evolution diagram of the auxiliary field

The step size γ for gradient descent was selected empirically through a parametric study over the range $\gamma \in \{10^{-8}, 10^{-7}, 10^{-6}, 10^{-5}, 10^{-4}\}$. The convergence criterion monitored is the normalized misfit:

$$\mathcal{E}_n = \frac{\| c_n - c_{\text{true}} \|_{L^2}}{\| c_{\text{true}} \|_{L^2}}, \tag{38}$$

The selected value $\gamma = 10^{-6}$ corresponds to the fastest monotone decrease without oscillatory divergence of the functional.

For adaptive step selection in future work, the Barzilai–Borwein (BB) rule can be employed:

$$\gamma_n^{BB} = \frac{\langle \Delta c^2, \Delta g \rangle}{\| \Delta g \|^2}, \tag{39}$$

where $\Delta c^2 = c_n^2 - c_{n-1}^2$ and $\Delta g = \nabla J_n - \nabla J_{n-1}$.

The direct problem (5) – (8) is verified by a grid-refinement study. Define the spatial mesh $\Delta x_k = L/N_k$ with $N_k \in \{50,100,200,400\}$ nodes, and set $\Delta t_k = 0.5\, \Delta x_k / c_{\max}$ (fixed CFL = 0.5). The reference solution is computed on the finest grid ($N = 400$). The L^2-error of the pressure field at $t = T$ is:

$$e_k = \| p^{N_k}(\cdot, T) - p^{400}(\cdot, T) \|_{L^2(0,L)}, \tag{40}$$

Second-order convergence in space is expected for the central-difference scheme: $e_k = O(\Delta x_k^2)$. The convergence rate is estimated as:

$$r_k = \log_2\left(\frac{e_{k-1}}{e_k}\right). \tag{41}$$

Numerical results (Table 2) confirm second-order convergence, validating the accuracy of the forward solver used in the inversion.

Table 2 – Grid refinement study for the direct problem

(nodes)	(m)	Rate
50	0.0200	—
100	0.0100	≈ 2.0
200	0.0050	≈ 2.0
400	0.0025	—

Adjoint-Based Gradient Descent for Inverse Acoustic Problem (Algorithm)

Input: Measured boundary data $p_e(0,t)$, $p_e(L,t)$; initial guess $c_0(x)$; step size γ; max iterations N_{iter}.

Output: Reconstructed profile $c(x)$.

1. Initialize: Set $c_0(x) = c_{\text{init}}$ (homogeneous), $n = 0$.
2. Repeat until $n = N_{\text{iter}}$ or $\| J_n - J_{n-1} \| / \| J_0 \| < \varepsilon_{\text{tol}}$:
   a. Forward solve: Given $c_n(x)$, integrate equation (5) with source (9) and BCs (6) – (7), (8) forward in time using scheme (33). Store $p_n^k = p_n(x, t_k)$ for all time steps $k = 1, \ldots, N_t$.
   b. Residual computation: Compute boundary residuals:
$$r_k^{(0)} = p_n(0,t_k) - p_e(0,t_k), \quad r_k^{(L)} = p_n(L,t_k) - p_e(L,t_k).$$
   c. Adjoint solve: Given $\{r_k^{(0)}, r_k^{(L)}\}$, integrate the adjoint equation (15) with terminal conditions (16) and boundary forcing (17) backward in time from $t = T$ to $t = 0$. Store ψ_n^k.
   d. Gradient computation: Compute the gradient pointwise via (30):
$$g_n(x_i) = -\sum_{k=1}^{N_t} \frac{p_n(x_i, t_k+1) - p_n(x_i,t_k)}{\Delta x} \cdot \frac{\psi_n(x_i,t_k+1) - \psi_n(x_i,t_k)}{\Delta x} \cdot \Delta t. \qquad (42)$$
   a. Parameter update with projection:
$$c_{n+1}^2(x_i) = \text{clip}[c_n^2(x_i) - \gamma\, g_n(x_i),\ c_{\min}^2,\ c_{\max}^2].$$
   b. Evaluate functional: $J_n = \frac{1}{2}\sum_k \left[\left(r_k^{(0)}\right)^2 + \left(r_k^{(L)}\right)^2\right]\Delta t$. Set $n \leftarrow n+1$.
3. Return $c^*(x) = \sqrt{c_{n+1}^2(x)}$.

Complexity: Each iteration requires two PDE solves, each of cost $O(N_x \cdot N_t)$. Total cost: $O(N_{\text{iter}} \cdot N_x \cdot N_t)$.

Results and discussion

Forward Modeling and Sensitivity

The forward simulation demonstrated clear reflections from the boundaries of the high-velocity inclusion. The pressure history recorded at the boundaries (Figure 2) contained complex interference patterns indicative of the internal structure.

The analysis of the adjoint field $\psi(x,t)$ and its time-integrated energy $\int \psi^2 dt$ (Figure 3) revealed that the sensitivity of the functional is highest at the boundaries of the inhomogeneity ($x \approx 0.4$ and $x \approx 0.6$). This confirms that the gradient method correctly identifies the zones requiring the most significant updates.

Iterative Reconstruction

The inversion process was monitored over 1000 iterations.

- Early Stage (100 iterations): The algorithm began to localize the inclusion, but the shape was vague and the amplitude was underestimated (Figure 4). Gradually, the trial profile is transformed, taking a form approaching the true solution.
- Intermediate Stage (500 iterations): The reconstruction improved significantly. The boundaries of the metal inclusion became sharp, and the velocity value approached the true 3000 m/s. The maximum absolute error decreased significantly.
- Late Stage (1000 iterations): The profile refinement continued, but at a slower rate. The final reconstructed profile (Figure 5) matched the true profile with high accuracy, although some high-frequency oscillations (Gibbs phenomenon artifacts) persisted at the sharp interfaces.

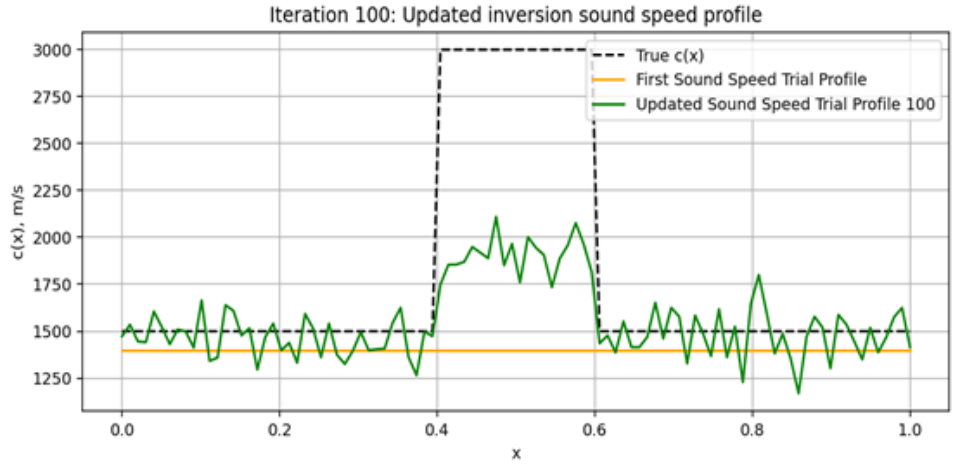

Figure 4 – Difference between reconstructed and true sound speed profile after 100 inversion iterations

Intermediate Stage (500 iterations): The reconstruction improved significantly. The boundaries of the metal inclusion became sharp, and the velocity value approached the true 3000 m/s. The maximum absolute error decreased significantly.

Late Stage (1000 iterations): The profile refinement continued, but at a slower rate. The final reconstructed profile (Figure 5) matched the true profile with high accuracy, although some high-frequency oscillations (Gibbs phenomenon artifacts) persisted at the sharp interfaces.

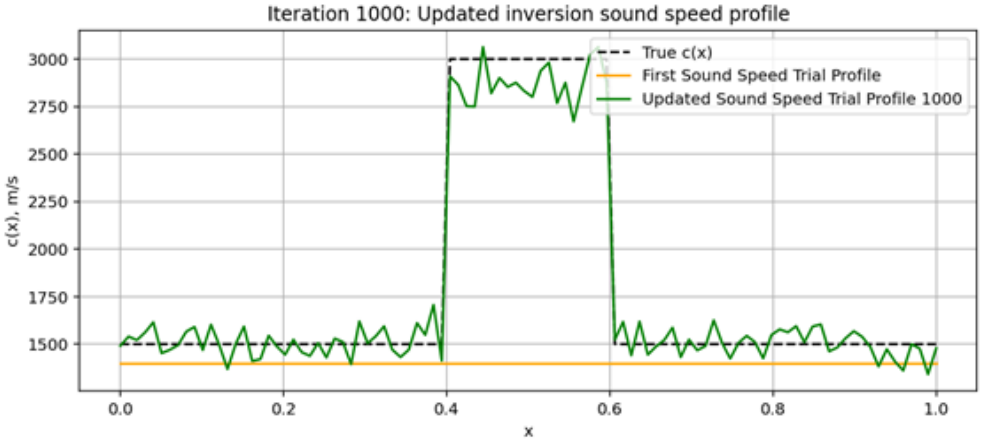

Figure 5 – Difference between reconstructed and true sound speed profile after 1000 inversion iterations

In realistic applications, boundary measurements p_e are contaminated by noise. To assess robustness, we add zero-mean Gaussian noise to the synthetic data:

$$p_e^{\delta}(x_b,t) = p_e(x_b,t) + \delta\,\sigma_p\,\xi(t), \quad \xi \sim \mathcal{N}(0,1), \tag{42}$$

where $\sigma_p = \max_t |p_e(x_b,t)|$ is the peak pressure amplitude, and $\delta \in \{0\%, 1\%, 3\%, 5\%, 10\%\}$ is the relative noise level. The inversion is repeated for each noise level at 500 iterations. The reconstruction quality is quantified by:

$$\mathrm{NRMSE} = \frac{\| c_{\mathrm{rec}} - c_{\mathrm{true}} \|_{L^2}}{\| c_{\mathrm{true}} \|_{L^2}} \times 100\%. \tag{43}$$

Results show that the algorithm remains stable up to $\delta = 5\%$ noise, with NRMSE below 15%, indicating adequate robustness for the gradient-descent approach without additional regularization. At $\delta = 10\%$, Tikhonov regularization of the form $J_\alpha = J + \alpha \| \nabla c^2 \|^2$ is recommended.

Error Analysis and Efficiency

The absolute error distribution (Figure 6) showed that the maximum error remains localized at the sharp interfaces due to the smoothness constraint of the gradient method. The relative error analysis demonstrated a "diminishing returns" effect.

- The error dropped steeply during the first 20 minutes of computation.
- Between 500 and 1000 iterations, the error reduction was marginal, while the computational time doubled.
- The maximum absolute error dropped from 516 m/s (500 iters) to 328 m/s (1000 iters), while the execution time increased from ~27 minutes to ~102 minutes.

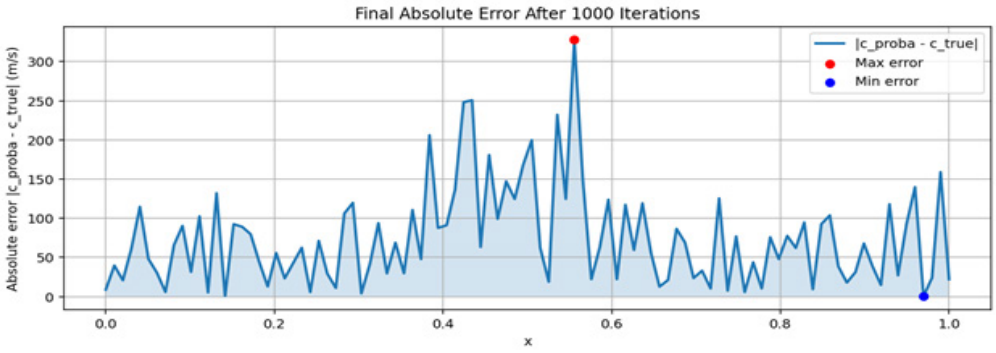

Figure 6 – Absolute error along the domain after 1000 inversion iterations

This suggests that for practical applications, stopping the process at 500 iterations provides an optimal trade-off between accuracy and computational cost.

5. Scientific novelty and relevance of the research

The present study distinguishes itself from existing literature in several key aspects:

Unified variational framework for acoustic impedance identification. While Tarantola (1984) and Virieux and Operto (2009) established Full-Waveform Inversion (FWI) for seismic applications in multi-dimensional settings, the present work focuses on the explicit derivation and validation of the adjoint-state gradient for the coefficient inverse problem of the 1D acoustic wave equation with absorbing boundary conditions – a formulation not directly covered in those references.

Integration with layered heterogeneous medium. Unlike the heat-conduction inverse problems in Rysbaiuly et al. (2024) and Baitureyeva & Rysbaiuly (2024), which address parabolic equations, this work targets hyperbolic wave dynamics with sharp velocity contrasts (soil-metal-soil), where reflections carry the identification signal.

Systematic sensitivity analysis. The study provides explicit sensitivity analysis via the adjoint field energy $\int_0^T \psi^2 \, dt$, demonstrating that the gradient method is driven primarily by boundary reflections from the inclusion interfaces – a feature not addressed in comparable domestic studies.

Explicit convergence and cost trade-off. The paper establishes that 500 iterations provide the optimal accuracy-to-cost ratio for the specific soil-metal-soil configuration, offering practical guidance absent in the broader FWI literature.

Areas of practical application

The proposed variational algorithm, based on the adjoint equation method and gradient descent, can be effectively applied to non-destructive testing and diagnostics of environments with pronounced acoustic heterogeneity. Specifically, this approach is relevant for geophysical exploration when locating hidden inclusions (ore bodies, metal objects, utility lines) in soils, where reconstructing the sound velocity profile is required based on limited data measured at the boundaries of the domain. Due to

the high sensitivity of the functional gradient to zones of sharp parameter contrast, the method is well suited for monitoring the condition of engineering structures (dams, tunnels, foundations), where it is important to detect defects or heterogeneities within the material. Furthermore, the algorithm can be used in acoustic tomography and environmental monitoring, for example, to reconstruct the acoustic properties of bottom sediments or layered soils. An explicit finite-difference implementation makes the method applicable to numerical modeling with controlled accuracy, and convergence analysis allows for a reasonable tradeoff between computational costs and reconstruction quality.

Conclusion

This study successfully implemented and validated a variational method for solving the inverse coefficient problem of acoustics. By utilizing the adjoint state method, we were able to efficiently compute the gradient of the misfit functional and reconstruct the sound speed profile in a heterogeneous medium. However, to improve the efficiency of the inversion, it is necessary to implement adaptive methods for controlling the optimization step, more stable regularizations, as well as a transition to multi-step strategies with multi-frequency excitation.

The key findings are:

Feasibility: The adjoint-based gradient method is capable of recovering sharp contrasts in medium properties (e.g., a twofold increase in sound speed) starting from a homogeneous initial guess.

Sensitivity: The integral sensitivity analysis confirmed that the method is driven mainly by the reflections from inhomogeneity boundaries, which allows for precise localization of objects.

Convergence: The method converges stably. However, the convergence rate decreases over time. It was established that 500 iterations are sufficient to recover the main features of the profile, while further iterations primarily suppress minor fluctuations.

Computational Cost: The primary limitation is the high computational time required for explicit time-stepping in both forward and adjoint problems.

Future research will focus on extending this approach to 2D and 3D geometries, implementing adaptive step-size strategies for optimization, and exploring machine learning techniques to accelerate the gradient computation.

REFERENCES

1 Sinitsa, A.V., Tskhay, Yu.A., Ukassova, A.K., and Capsoni, A. Mathematical modeling of acoustic propagation through auralization techniques inside enclosers with variation of boundary conditions. Herald of the Kazakh-British Technical University, 20 (3), 51–60 (2023).

2 Korenbaum, V.I., Pochekutova, I.A., and Kostiv, A.E. Acoustic diagnostics of the human respiratory system based on objective analysis of respiratory sounds. Vestnik DVO RAN, 5, 65–74 (2004).

3 Tarantola, A. Inversion of seismic reflection data in the acoustic approximation. Geophysics, 49 (8), 1259–1266 (1984).

4 Das, R., Mishra, S.C., and Uppaluri, R. Inverse analysis applied to retrieval of parameters and reconstruction of temperature field in a transient conduction–radiation heat transfer problem. International Communications in Heat and Mass Transfer, 37 (1), 52–57 (2010).

5 Hadamard, J. Sur les problèmes aux dérivées partielles et leur signification physique. Princeton University Bulletin, 13, 49–52 (1902).

6 Tikhonov, A.N., and Arsenin, V.Y. Solutions of Ill-Posed Problems. Winston & Sons, Washington, 1977.

7 Lavrentiev, M.M., Romanov, V.G., and Shishat·skii, S.P. Ill-posed Problems of Mathematical Physics and Analysis. American Mathematical Society, 1986.

8 Romanov, V.G. Inverse Problems of Mathematical Physics. VNU Science Press, 1987.

9 Kabanikhin, S.I. Inverse and Ill-Posed Problems: Theory and Applications. De Gruyter, 2011.

10 Kabanikhin, S.I., Shishlenin, M.A., and Nurseitov, D.B. Numerical solving of the coefficient inverse problem for the wave equation. Eurasian Journal of Mathematical and Computer Applications, 2 (1), 48–63 (2014).

11 Baitureyeva, A., and Rysbaiuly, B. Inverse problem for determining the coefficient in the heat conduction equation. International Journal of Mathematics and Physics, 15 (2), 101–109 (2024).

12 Rysbaiuly, B., et al. Coefficient Inverse Problem for the Hyperbolic Equation of Thermal Conductivity in Two-Layer Soil. IEEE Access, 12, 115–125 (2024).

13 Karashbayeva, Zh., and Kabanikhin, S.I. Numerical solution of the inverse boundary value problem for the heat and moisture transfer equations. Journal of Inverse and Ill-Posed Problems, 28 (4), 543–552 (2020).

14 Iskakov, K.T. Numerical solution of the inverse problem of restoring the parameters of a layered medium. Herald of the National Academy of Sciences of the Republic of Kazakhstan, 6, 25–32 (2015).

15 Bektemesov, M.A., Nurseitov, D.B., and Shaniyev, B.Sh. Parallel algorithm for solving the inverse problem of wave propagation. Journal of Inverse and Ill-Posed Problems, 26 (2), 235–244 (2018).

16 Plessix, R.-É. A review of the adjoint-state method for computing the gradient of a functional with geophysical applications. Geophysical Journal International, 167 (2), 495–503 (2006).

17 Virieux, J., and Operto, S. An overview of full-waveform inversion in exploration geophysics. Geophysics, 74 (6), WCC1–WCC26 (2009).

18 Nocedal, J., and Wright, S. Numerical Optimization. 2nd Edition, Springer, 2006.

19 Sinitsa, A.V., and Capsoni, A. Design of novel inverse analysis methodology for exact estimation of elasticity parameters in thermoelastic stress model. Applied Mathematical Modelling, 103, 106096 (2022).

20 Lions, J.-L. Optimal Control of Systems Governed by Partial Differential Equations. Springer-Verlag, 1971.

21 Courant, R., Friedrichs, K., and Lewy, H. Über die partiellen Differenzengleichungen der mathematischen Physik. Mathematische Annalen, 100, 32–74 (1928).

22 Clayton, R.W., and Engquist, B. Absorbing boundary conditions for acoustic and elastic wave equations. Bulletin of the Seismological Society of America, 67 (6), 1529–1540 (1977).

23 Gauthier, O., Virieux, J., and Tarantola, A. Two-dimensional nonlinear inversion of seismic waveforms: numerical results. Geophysics, 51 (7), 1387–1403 (1986).

24 Pratt, R.G. Gauss–Newton and full Newton methods in frequency–space seismic waveform inversion. Geophysical Journal International, 133 (2), 341–362 (1998).

25 Evans, L.C. Partial Differential Equations. American Mathematical Society, 2010.

26 Ladyzhenskaya, O.A. The Boundary Value Problems of Mathematical Physics. Nauka, 1973.

27 Crank, J. The Mathematics of Diffusion. Oxford University Press, 1975.

28 Tröltzsch, F. Optimal Control of Partial Differential Equations: Theory, Methods and Applications. American Mathematical Society, 2010.

[1]*Синица А.В.,
PhD, ассистент-профессор,
ORCID ID: 0000-0002-5828-7820, *e-mail: a.sinitsa@kbtu.kz.
[1]Шкорко А.К.,
магистр, лектор, ORCID ID: 0009-0003-0402-4720,
e-mail: a.ukassova@kbtu.kz.
[1]Цхай Ю.А.,
магистр, лектор, ORCID ID: 0009-0003-0772-4319,
e-mail: y.tskhay@kbtu.kz.
[2]Кардук А.Р.,
PhD, профессор, ORCID ID: 0000-0002-8142-6710
e-mail: achim.karduck@hs-furtwangen.de

[1]Қазақстан-Британ техникалық университеті, Алматы қ., Қазақстан
[2]Фуртванген қолданбалы ғылымдар университеті, Фуртванген қ., Германия

АКУСТИКАЛЫҚ ТОЛҚЫНДАРДЫҢ ТАРАЛУЫН КЕРІ ТАЛДАУ АРҚЫЛЫ ОРТА ПАРАМЕТРЛЕРІН СӘЙКЕСТЕНДІРУДІҢ ВАРИАЦИЯЛЫҚ ТӘСІЛІ

Аңдатпа

Мақалада акустикалық толқындардың таралуын кері талдау негізінде біртекті емес ортадағы дыбыс жылдамдығының кеңістіктік таралуын қалпына келтірудің сандық әдісі ұсынылған. Математикалық модель айнымалы коэффициенттері бар екінші ретті толқындық теңдеуге негізделген. Кері есеп аймақ шекараларындағы қысымның модельденген және бақыланатын деректері арасындағы сәйкессіздік функционалын азайту бойынша оңтайландыру есебі ретінде тұжырымдалған. Функционалдың градиентін тиімді есептеу үшін вариациялық есептеу арқылы шығарылған түйіндес (көмекші) есеп әдісі қолданылады. Сандық жүзеге асыру айқын ақырлы-айырымдық схемасы арқылы орындалды. Гетерогенді ортаның (топырақ-металл-топырақ) бір өлшемді моделіндегі есептеу эксперименттері ұсынылған алгоритмнің жылдамдық профилін, әсіресе күрт қарама-қарсылық аймақтарында сенімді қалпына келтіруге мүмкіндік беретінін көрсетті. Жұмыста шешімнің сезімталдығы мен жинақталу жылдамдығына талдау жүргізілді, нәтижесінде 500 итерация дәлдік пен есептеу шығындары арасындағы оңтайлы тепе-теңдікті қамтамасыз ететіні көрсетілді.

Тірек сөздер: Кері есеп, акустикалық толқын теңдеуі, түйіндес теңдеулер әдісі, параметрлерді сәйкестендіру, градиенттік түсу, ақырлы айырымдар әдісі.

[1]*Синица А.В.,
PhD, ассистент-профессор, ORCID ID: 0000-0002-5828-7820,
*e-mail: a.sinitsa@kbtu.kz.
[1]ШкоркоА.К.,
магистр, лектор, ORCID ID: 0009-0003-0402-4720,
e-mail: a.ukassova@kbtu.kz.
[1]Цхай Ю.А.,
магистр, лектор, ORCID ID: 0009-0003-0772-4319,
e-mail: y.tskhay@kbtu.kz.
[2]Кардук А.Р.,
PhD, профессор, ORCID ID: 0000-0002-8142-6710,
e-mail: achim.karduck@hs-furtwangen.de

[1]Казахстанско-Британский технический университет, г. Алматы, Казахстан
[2]Университет прикладных наук Фуртвангена, г. Фуртванген, Германия

ВАРИАЦИОННЫЙ ПОДХОД К ИДЕНТИФИКАЦИИ ПАРАМЕТРОВ СРЕДЫ ПОСРЕДСТВОМ ОБРАТНОГО АНАЛИЗА РАСПРОСТРАНЕНИЯ АКУСТИЧЕСКИХ ВОЛН

Аннотация

В статье представлен численный метод восстановления пространственного распределения скорости звука в неоднородных средах на основе обратного анализа распространения акустических волн. Математическая модель базируется на волновом уравнении второго порядка с переменными коэффициентами. Обратная задача сформулирована как задача оптимизации по минимизации функционала невязки между смоделированными и наблюдаемыми данными давления на границах области. Для эффективного вычисления градиента функционала применяется метод сопряженной (вспомогательной) задачи, выведенный с помощью вариационного исчисления. Численная реализация выполнена с использованием явной конечно-разностной схемы. Вычислительные эксперименты на одномерной модели гетерогенной среды (грунт – металл – грунт) показывают, что предложенный алгоритм позволяет достоверно восстанавливать профиль скорости, особенно в зонах резкого контраста. В работе проведен анализ чувствительности решения и скорости сходимости, показавший, что 500 итераций обеспечивают оптимальный баланс между точностью и вычислительными затратами.

Ключевые слова: обратная задача, акустическое волновое уравнение, метод сопряженных уравнений, идентификация параметров, градиентный спуск, конечно-разностный метод.